The Application of Exciton Theory to the Determination of the Absolute Configurations of Inorganic Complexes

B. BOSNICH

William Ramsay and Ralph Forster Laboratories, University College, London, W.C.1, England

Circular dichroism is a property associated with dissymmetric molecules. It is defined as the difference $\epsilon_l - \epsilon_r$, where ϵ_l and ϵ_r are the molar extinction coefficients of left- and right-handed circularly polarized light, respectively. The property is therefore intimately connected with the spectroscopic transitions of optically active molecules. The sign of the circular dichroism for a particular electronic transition is directly related to the absolute configuration of the molecule and, in principle, it should be possible to derive one from a knowledge of the other.

There are currently a number of theoretical models for the origins of optical activity, perhaps the most notable of which we discuss here, the exciton theory. This model has its origins in the early classical coupled oscillator theories of Born, Oseen, and Kuhn.[1-3] These workers recognized, as others had before them, that, in order to generate optical activity by the absorption of light, electronic displacements must occur which induce simultaneous *collinear* electric and magnetic transition dipole moments in the media. Since, in a pictorial sense, an electric transition dipole moment is produced by a linear displacement of charge and a magnetic transition dipole moment is produced by a circulation of charge, optically active transitions involve helical displacements of charge. By definition a right-handed helical displacement produces positive circular dichroism ($\epsilon_l > \epsilon_r$) and a left-handed helical displacement produces negative circular dichroism ($\epsilon_r > \epsilon_l$). Their conception of dissymmetric coupled oscillators for this purpose was the classical precursor to the main part of the polarizability theory of Kirkwood[4] and the exciton formulation of Moffitt.[5]

Both theories are quantum mechanical, and what is particularly interesting about them is that, in principle, they offer a straightforward, purely spectroscopic, method for determining the absolute configurations of molecules. In other words, we are offered a method of determining the chirality (handedness) of a molecule without reference to or knowledge of the independently determined absolute configuration of any other molecule; in fact, all we need is the circular dichroism shown by certain electronic transitions of known polarization. As might be expected, however, few optically active molecules are at present susceptible to this treatment, although it has been applied with success to a number of

organic systems. In particular, independent determinations of the absolute configurations of certain simple coupled π-electron systems[6,7] and of helical polypeptides[8] support the predictions of the exciton theory.

For inorganic complexes the method can be applied to the important class of dissymmetric coordination compounds containing conjugated ligands which are typified by the three strongly coordinating bidentate ligands, *o*-phenanthroline (phen), 2,2'-bipyridyl (bipy), and the acetylacetonate ion (acac). The recent X-ray diffraction determination[9] of the absolute configuration of the $(-)$-$[Fe(phen)_3]^{2+}$ ion has confirmed the validity of the method when applied to complexes, and because now most of the important members of this class of complexes have been investigated, it seems opportune to review this information and to formulate general rules for the assignment of their absolute configurations.

The $\pi \rightarrow \pi^*$ transitions of the free ligands phen, bipy, and acac are polarized in the molecular plane and are directed either along the short axis (z) or the long axis (x) of the ligands (Figure 1). Upon complex formation these transitions remain largely unmodified.[10] Complexes containing only one of these conjugated ligands, as in, for example, the dissymmetric ion $[Co(en)_2phen]^{3+}$ (en = ethylenediamine), show comparatively weak circular dichroism in the regions of the $\pi \rightarrow \pi^*$ ligand transitions.[10] When two or more conjugated ligands are present, the circular dichroism shown by the short-axis-polarized ligand transitions remains weak, but that associated with the long-axis-polarized transitions is exceedingly strong. These observations agree with the expectations of the exciton theory of optical activity which assumes that the circular dichroism is produced by electrostatic coupling of the electric transition dipole moments which are essentially localized on the ligands. In an octahedral complex, the short-axis-polarized ligand transitions couple to give only electric transition dipole moments in the zero order and therefore cannot give rise to exciton optical activity. The weak circular dichroism associated with these transitions is due to higher order dissymmetric perturbations. The long-axis-polarized transitions, however, couple to give paral-

(1) M. Born, *Physik. Z.*, **16**, 251 (1915).
(2) C. W. Oseen, *ibid.*, **16**, 1 (1915).
(3) W. Kuhn, *Z. Physik. Chem.*, **B4**, 14 (1929).
(4) J. G. Kirkwood, *J. Chem. Phys.*, **5**, 479 (1937).
(5) W. Moffitt, *ibid.*, **25**, 467 (1956).

(6) L. S. Forster, A. Moscowitz, J. G. Berger, and K. Mislow, *J. Amer. Chem. Soc.*, **84**, 4353 (1962).
(7) R. Grinter and S. F. Mason, *Trans. Faraday Soc.*, **60**, 274 (1964).
(8) G. Holzworth and P. Doty, *J. Amer. Chem. Soc.*, **87**, 218 (1965).
(9) D. H. Templeton, A. Zalkin, and T. Ueki, *Acta Cryst.*, **21**, A154 (1966).
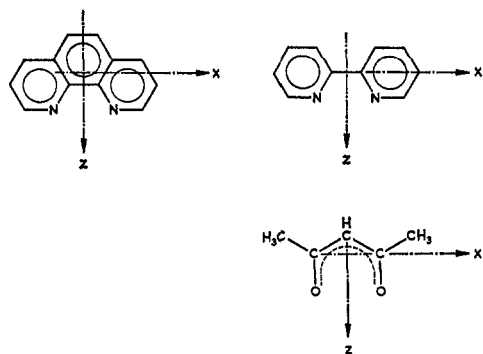(10) J. Hidaka and B. E. Douglas, *Inorg. Chem.*, **3**, 1180 (1964).

Figure 1. The o-phenanthroline and 2,2'-bipyridyl molecules and the acetylacetonate ion showing the long (x) and short (z) axes.

lel electric and magnetic transition dipole moments in the zero order, and calculation shows that the rotational strengths produced by this mechanism are very large and can account for the experimentally observed circular dichroism. It is this circular dichroism associated with the long-axis-polarized transitions of the (complexed) ligands which allows for the nonempirical determination of the absolute configurations of octahedral metal complexes, and the discussion which follows will mainly concern itself with these transitions. Molecular orbital calculations, polarized crystal spectra, and circular dichroism data indicate that the first long-axis-polarized $\pi \rightarrow \pi^*$ transitions of the o-phenanthroline[11-15] and the 2,2'-bipyridyl[10,16,17] molecules and of acetylacetonate ions[18,19] occur at ca. 38,000, 34,500, and 35,000 cm.$^{-1}$, respectively.

A Physical Model

Transition metal complexes of the type we will discuss have three types of electronic transitions: those which are essentially localized on the metal, those which occur between the metal and ligands, and those which are essentially localized on the ligands. The absorption bands associated with these transitions all carry some circular dichroism, but we will only consider the optical activity arising from the coupling of electric transition dipoles of the ligands. The justification for this ultimately rests on experiment, although there are sound theoretical reasons for the procedure.

For the present purposes it is convenient to divide optically active metal complexes into five categories: (a) the identical tris-bidentate case, e.g., [M(phen)$_3$]$^{n+}$, (b) the identical cis bis-bidentate case, e.g., cis-[M(phen)$_2$X$_2$]$^{n+}$, (c) the nonidentical cis bis-bidentate

case, e.g., cis-[M(phen)(bipy)X$_2$]$^{n+}$, (d) the tris-bidentate case with two different ligands, e.g., [M(phen)$_2$bipy]$^{n+}$ or [M(bipy)$_2$phen]$^{n+}$, and (e) the tris-bidentate case with three different ligands, e.g., [M(phen)(bipy)acac]$^{n+}$. The exciton optical activity of all these cases can be calculated, except that in case e analytical solutions are generally not possible, although for most cases the results will be very similar to those for case d. The reader who is interested in the precise form of the solutions will find them in Table I. Similarly the basic formalism and general assumptions involved in the derivation of the solutions are described in the last section. In this section we shall try to show by means of somewhat simplified models how the exciton circular dichroism is generated in these systems. We take the identical tris-bidentate case [M(phen)$_3$]$^{n+}$ as a representative example.

In a classical sense an electric transition dipole moment is induced in a molecule when there is a translational motion of charge during the absorption of light. The long-axis-polarized $\pi \rightarrow \pi^*$ transition of the phen molecule involves an oscillating displacement of the π electrons along the x axis (Figure 1). This transition by itself cannot produce circular dichroism because, as we have stated earlier, circular dichroism is produced only by transitions which involve both a translation and circulation of charge. This is why we observe[10] very little circular dichroism under the long-axis-polarized phen transition in [Co(en)$_2$phen]$^{3+}$; what little there is is due to higher order dissymmetric perturbations. When three phen molecules are coordinated octahedrally to a metal atom, the charge oscillations remain linear in each molecule but, provided the adjacent electric transition dipole moments can interact, a photon can cause all three molecules to be excited and each is no longer independent of the other. Therefore the true stationary states (wave functions) of the system must take this into account. Provided there is no electron exchange (charge transfer) between the phen molecules in [M(phen)$_3$]$^{n+}$, we may specify the stationary states of the system as simple product functions. Thus, the ground-state function is written as $\Psi_0 = \chi_1\chi_2\chi_3$ and the three locally excited-state functions are written as $\chi_1'\chi_2\chi_3$, $\chi_1\chi_2'\chi_3$, and $\chi_1\chi_2\chi_3'$, where the numbers 1, 2, 3 label each phen molecule, χ is the ground-state function of phen, and the primes refer to excited-state functions of phen. Since the three locally excited states are degenerate and not independent, the true stationary state is specified by linear combinations of them. These linear combinations in essence describe the phase relationships between the dipole excitation vectors of each phen molecule. It turns out (Table I) that in the [M(phen)$_3$]$^{n+}$ system the three coupling modes (phase combinations) for the long-axis-polarized transitions are symmetry determined. Accordingly, the three exciton transitions are labeled $\Psi_0 \rightarrow \Psi_{A_2}$, $\Psi_0 \rightarrow \Psi_E^1$, and $\Psi_0 \rightarrow \Psi_E^2$; the last two are degenerate. These three coupling modes are shown on the left in Figure 2 where the arrows represent the directions of the long-axis-polarized $\pi \rightarrow \pi^*$

(11) D. S. McClure, J. Chem. Phys., **25**, 481 (1956).

(12) T. Azumi and S. McGlynn, ibid., **37**, 2413 (1962).

(13) D. P. Craig and R. D. Gordon, Proc. Roy. Soc. (London), **A288**, 69 (1965).

(14) A. J. McCaffery, S. F. Mason, and B. J. Norman, Proc. Chem. Soc., 259 (1964).

(15) A. J. McCaffery and S. F. Mason, ibid., 211 (1963).

(16) T. M. Dunn, J. R. Gott, and C. Zauli, Boll. Sci. Fac. Chim. Ind. Bologna, **18**, 210 (1960).

(17) R. Coffman and D. S. McClure, Can. J. Chem., **36**, 48 (1958).

(18) E. Larsen, S. F. Mason, and G. H. Searle, Acta Chem. Scand., **20**, 191 (1966).

(19) L. S. Forster, J. Amer. Chem. Soc., **86**, 3001 (1964).

Table

Example	Exciton wave functions	Energies
Case a $[M(phen)_3]^{n+}$ $[M(bipy)_3]^{n+}$ $[M(acac)_3]^{n+}$	$\Psi_0 = \chi_1\chi_2\chi_3$ $\Psi_{A_2} = (1/\sqrt{3})(\chi_1'\chi_2\chi_3 + \chi_1\chi_2'\chi_3 + \chi_1\chi_2\chi_3')$ $\Psi_E{}^1 = (1/\sqrt{6})(2\chi_1'\chi_2\chi_3 - \chi_1\chi_2'\chi_3 - \chi_1\chi_2\chi_3')$ $\Psi_E{}^2 = (1/\sqrt{2})(\chi_1\chi_2'\chi_3 - \chi_1\chi_2\chi_3')$	0 $E_{A_2} = \Delta E + 2V_{12}$ $E_E = \Delta E - V_{12}$ $E_E = \Delta E - V_{12}$
Case b $[M(phen)_2X_2]^{n+}$ $[M(bipy)_2X_2]^{n+}$ $[M(acac)_2X_2]^{n+}$	$\Psi_0 = \chi_1\chi_2$ $\Psi_A = (1/\sqrt{2})(\chi_1'\chi_2 + \chi_1\chi_2')$ $\Psi_B = (1/\sqrt{2})(\chi_1'\chi_2 - \chi_1\chi_2')$	0 $E_A = \Delta E + V_{12}$ $E_B = \Delta E - V_{12}$
Case c $[M(phen)(bipy)X_2]^{n+}$ $[M(phen)(acac)X_2]^{n+}$ $[M(bipy)(acac)X_2]^{n+}$	$\Psi_0 = \chi_1\varphi_2$ $\Psi^+ = C_A{}^+\chi_1'\varphi_2 + C_B{}^+\chi_1\varphi_2'$ $\Psi^- = C_A{}^-\chi_1'\varphi_2 + C_B{}^-\chi_1\varphi_2'$	0 $2E^+ = \Delta E_1 + \Delta E_2 + K$ $2E^- = \Delta E_1 + \Delta E_2 - K$
Case d $[M(phen)_2bipy]^{n+}$ $[M(bipy)_2phen]^{n+}$ $[M(phen)_2acac]^{n+}$ etc.	$\Psi_0 = \chi_1\chi_2\varphi_3$ $\Psi_A = (1/\sqrt{2})(\chi_1'\chi_2\varphi_3 - \chi_1\chi_2'\varphi_3)$ $\Psi_B{}^+ = C_1{}^+\{(1/\sqrt{2}(\chi_1'\chi_2\varphi_3 + \chi_1\chi_2'\varphi_3)\} + C_2{}^+\chi_1\chi_2\varphi_3'$ $\Psi_B{}^- = C_1{}^-\{(1/\sqrt{2})(\chi_1'\chi_2\varphi_3 + \chi_1\chi_2'\varphi_3\} + C_2{}^-\chi_1\chi_2\varphi_3'$	0 $E_A = \Delta E_1 - V_{12}$ $2E_B{}^+ = \Delta E_1 + \Delta E_3 + V_{12} + L$ $2E_B{}^- = \Delta E_1 + \Delta E_3 + V_{12} - L$

[a] All r's refer to the distance between the "center" of the excitation and the center of the metal. In case d the labels 1 and 2 refer to the identical ligands and 3 refers to the one that is different. The signs of the rotational strengths refer to absolute configurations
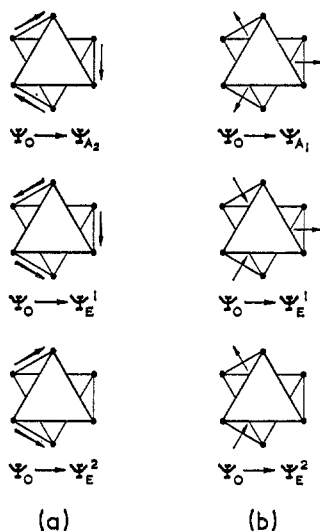

Figure 2. A diagrammatic representation of the three coupling modes of the long-axis-polarized ligand transitions (a) and the short-axis-polarized ligand transitions (b).

transitions of the phen molecules. We can now see how the exciton circular dichroism is generated.

Let us consider the $\Psi_0 \rightarrow \Psi_{A_2}$ transition. If the three linear vectors are added, there is a net resultant linear displacement along the threefold axis of the molecule (perpendicular to the plane of the paper). However, because the vectors are arranged like a three-bladed propellor, their combined effect also engenders a circulation of charge about the threefold axis which produces a magnetic moment (Lenz's law) along this axis. Thus the $\Psi_0 \rightarrow \Psi_{A_2}$ transition involves a helical displacement of charge along and about the threefold axis. For the particular absolute configuration shown in Figure 2, it will be seen that the screw sense of the $\Psi_0 \rightarrow \Psi_{A_2}$ transition is left handed, and hence this transition should give negative circular dichroism (Table I). The $\Psi_0 \rightarrow \Psi_E{}^2$ transition involves the excitation of only two of the phen molecules, and it will be seen that this coupling combination involves a right-handed helical displace-

ment of charge along and about the twofold axis (in the plane of the paper). The effect of the $\Psi_0 \rightarrow \Psi_E{}^1$ transition is more difficult to see, but calculation shows that it also involves a net right-handed helical displacement at right angles to the threefold and twofold axes of the molecule. Thus the "total" $\Psi_0 \rightarrow \Psi_E$ transition should give positive circular dichroism. It can be shown that the rotational strength of the $\Psi_0 \rightarrow \Psi_{A_2}$ transition is equal but opposite in sign to the $\Psi_0 \rightarrow \Psi_E$ excitation, and, were these two transitions of the same energy, the exciton rotational strength would vanish. The energies of the two transitions, however, are different because the interactions of the dipoles in the two coupling modes are different. We can see this in the following way.

The Ψ_{A_2} coupling mode involves the dipole vectors in an arrangement where they are essentially "head to head," whereas the $\Psi_E{}^2$ coupling mode (which is the same energy as $\Psi_E{}^1$) involves the dipoles in an essentially "head-to-tail" arrangement. Intuitive electrostatic considerations will suggest that the "head-to-head" arrangement is of higher energy than the "head-to-tail" arrangement. Thus for the particular absolute configuration shown in Figure 2, the $[M(phen)_3]^{n+}$ systems should show positive circular dichroism at lower energies and equal negative circular dichroism to higher energies in the regions of the long-axis-polarized $\pi \rightarrow \pi^*$ transition of phen. In addition, it can be shown that the ordinary absorption of the $\Psi_0 \rightarrow \Psi_{A_2}$ transition should be twice as strong as that of the $\Psi_0 \rightarrow \Psi_E$ transition if we assume that the absorption intensity is determined by the dipole strength (see Table I).

In the introduction we said that the short-axis-polarized phen transitions should not and do not show any exciton circular dichroism. The present simplified pictorial arguments help show why this is so. It can be shown that the short-axis-polarized transitions should couple to give two transitions, $\Psi_0 \rightarrow \Psi_{A_1}$ and the doubly degenerate $\Psi_0 \rightarrow \Psi_E$. The right-hand side of Figure 2 shows the electric dipole phase relationships for these

I^a

Dipole strength ($\Psi_0 \rightarrow \Psi_{\text{excited}}$)   Rotational strength ($\Psi_0 \rightarrow \Psi_{\text{excited}}$)

$$D_{A_2} = 2\rho^2$$
$$\{D_E = \rho^2$$

$$\mathfrak{R}_{A_2} = -\sqrt{2}\pi\bar{\nu}r\rho^2$$
$$\{\mathfrak{R}_E = +\sqrt{2}\pi\bar{\nu}r\rho^2$$

$$D_A = \frac{1}{2}\rho^2$$
$$D_B = \frac{3}{2}\rho^2$$

$$\mathfrak{R}_A = +(1/\sqrt{2})\pi\bar{\nu}r\rho^2$$
$$\mathfrak{R}_B = -(1\sqrt{2})\pi\bar{\nu}r\rho^2$$

$$D^+ = (C_A{}^+)^2\rho_1{}^2 + (C_B{}^+)^2\rho_2{}^2 + C_A{}^+C_B{}^+\rho_1\rho_2$$
$$D^- = (C_A{}^-)^2\rho_1{}^2 + (C_B{}^-)^2\rho_2{}^2 + C_A{}^-C_B{}^-\rho_1\rho_2$$

$$\mathfrak{R}^+ = -C_A{}^+C_B{}^+\pi\rho_1\rho_2(1/\sqrt{2})(\bar{\nu}_1r_1 + \bar{\nu}_2r_2)$$
$$\mathfrak{R}^- = -C_A{}^-C_B{}^-\pi\rho_1\rho_2(1/\sqrt{2})(\bar{\nu}_1r_1 + \bar{\nu}_2r_2)$$

$$D_A = \frac{1}{2}\rho_1{}^2$$
$$D_B{}^+ = (C_1{}^+)^2 \frac{3}{2}\rho_1{}^2 + (C_2{}^+)^2\rho_3{}^2 + C_1{}^+C_2{}^+\sqrt{2}\rho_1\rho_2$$
$$D_B{}^- = (C_1{}^-)^2 \frac{3}{2}\rho_1{}^2 + (C_2{}^-)^2\rho_3{}^2 + C_1{}^-C_2{}^-\sqrt{2}\rho_1\rho_2$$

$$\mathfrak{R}_A = +(1/\sqrt{2})\pi\bar{\nu}_1r_1\rho_1{}^2$$
$$\mathfrak{R}_B{}^+ = -(C_1{}^+)^2(1/\sqrt{2})\pi\bar{\nu}_1r_1\rho_1{}^2 - C_1{}^+C_2{}^+\pi\rho_1\rho_3(\bar{\nu}_1r_1 + \bar{\nu}_3r_3)$$
$$\mathfrak{R}_B{}^- = -(C_1{}^-)^2(1/\sqrt{2})\pi\bar{\nu}_1r_1\rho_1{}^2 - C_1{}^-C_2{}^-\pi\rho_1\rho_3(\bar{\nu}_1r_1 + \bar{\nu}_3r_3)$$

related to $(-)$-[Fe(phen)$_3$]$^{2+}$.

transitions. It is seen that the $\Psi_0 \rightarrow \Psi_{A_1}$ transition involves only an "outward" linear displacement of charge; in fact, the vector sum cancels and the transition is forbidden. The two $\Psi_0 \rightarrow \Psi_E$ coupling modes do give resultant linear displacements of charge and are allowed in electric dipole radiation fields. But in neither the $\Psi_0 \rightarrow \Psi_{A_1}$ nor the $\Psi_0 \rightarrow \Psi_E$ transition do the dipoles couple to give any circulation of charge to produce a magnetic dipole moment. It is for these reasons that the short-axis-polarized transitions should show no exciton circular dichroism.

In Figure 3 we show the absorption and circular dichroism spectra of $(+)$-[Ru(phen)$_3$](ClO$_4$)$_2$; there are three main regions of absorption. The group of moderately intense bands occurring in the 19,000–27,000-cm^{-1} region are charge-transfer transitions involving excitation of d$_\epsilon$ electrons of the metal to the antibonding π^* orbitals of the ligand. Transitions occurring in the 27,000–33,000-cm^{-1} region are dominated by the short-axis-polarized transitions, and the intense band centered at 38,000 cm^{-1} is the long-axis-polarized ligand transition. The circular dichroism associated with the long-axis-polarized transition is more than an order of magnitude greater than that associated with either the short-axis-polarized transitions or the charge-transfer bands. In addition, the 38,000-cm^{-1} band carries two circular dichroism bands which are almost equal and opposite in sign. These observations agree with the expectations of the exciton theory; thus, $(+)$-[Ru(phen)$_3$]$^{2+}$ ion has the absolute configuration shown in the inset of Figure 3. The $(-)$-[Fe(phen)$_3$]$^{2+}$ ion shows a similar plus–minus circular dichroism in the 38,000-cm^{-1} region, and the X-ray crystal structure determination of the absolute configuration confirms the predictions of the exciton theory. A similar pattern obtains for the [M(bipy)$_3$]$^{n+}$ systems.[10]

In both the tris(bipyridyl) and tris(o-phenanthroline) transition metal complexes the dipole strength criterion, namely that the higher energy exciton component
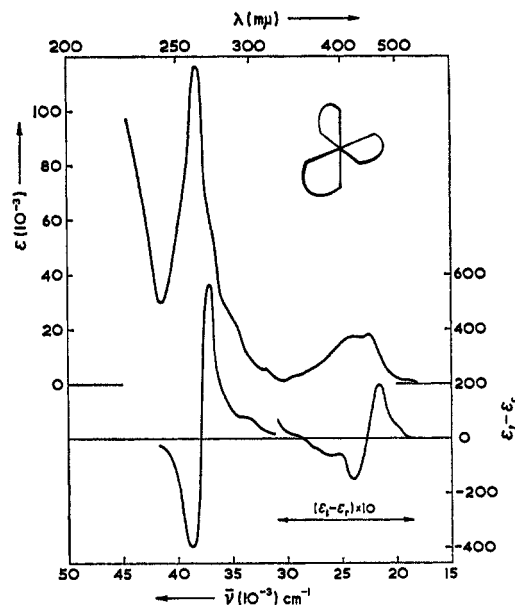

Figure 3. The absorption and circular dichroism spectra of $(+)$-[Ru(phen)$_3$](ClO$_4$)$_2$ in water solution and the predicted absolute configuration.

should be twice as intense as the lower energy component, is generally unreliable. This arises mainly because the long-axis-polarized transitions are heavily overlapped by other bands whose intensity and position vary with the metal and with the oxidation state of the same metal. The exciton circular dichroism bands also vary somewhat with regard to the relative intensities of the two exciton components and also with regard to their absolute magnitudes as the metal or oxidation state is changed. However, because the exciton circular dichroism in these complexes dominates the other circular dichroism bands, there is little difficulty in assigning the absolute configurations, although attempts to obtain a more quantitative comparison with theory are made difficult.
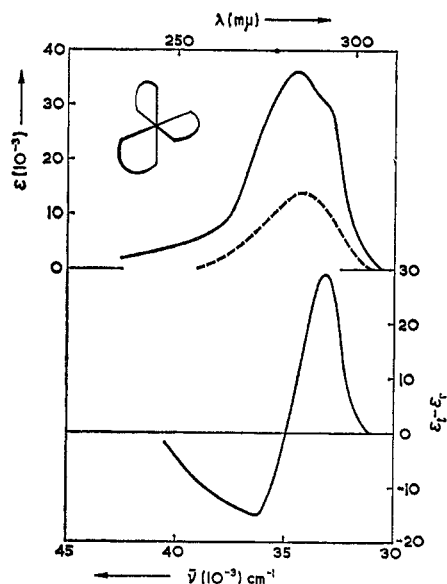
These complications are to some extent avoided in

Figure 4. The absorption spectrum of the acetylacetonate ion (- - - -) in water and the absorption and circular dichroism spectra of (+)-[Si(acac)₃]ClO₄ in water. The predicted absolute configuration is shown in the inset (data kindly supplied by S. F. Mason).

the case of the active [Si(acac)₃]⁺ ion which should show in the accessible spectral region only the long-axis-polarized transition due to the acetylacetonate ion. Figure 4 shows the absorption and associated circular dichroism spectra of the (+)-[Si(acac)₃]⁺ ion. The absorption spectrum is three times as intense as the corresponding absorption of the free acac ion. Further, the transition is split, with the higher energy band being more intense than the lower energy band and each of these components carrying circular dichroism which is nearly equal and opposite. All these observations are in semi-quantitative agreement with the expectations derived from assuming an exciton coupling scheme.

Similar arguments[20,21] to those used here for the $[M(phen)_3]^{n+}$ systems can be employed for other types of complexes. The analytical solutions for these other cases are collected in Table I and shown diagrammatically in Figure 5. Although the expressions for the rotational strengths are the same for $[M(phen)_2bipy]^{n+}$ and $[M(bipy)_2phen]^{n+}$, there are observational differences which are of significance. If the nonidentical chromophores did not couple, the rotational strength expressions would reduce to the ones given for case b, and we would expect a plus–minus pattern under the long-axis-polarized transition of phen in $[M(phen)_2bipy]^{n+}$ and a plus–minus circular dichroism pattern under the bipy long-axis-polarized absorption of $[M(bipy)_2phen]^{n+}$. If in both complexes there is nonidentical coupling, the circular dichroism pattern—shown in Figure 5—should be different. Thus these two complexes provide an experimental test for the importance of nonidentical coupling, which is the reason why two examples are given in Figure 5 for case d.

(20) B. Bosnich, *Inorg. Chem.*, **7**, 178 (1968).
(21) B. Bosnich, *ibid.*, **7**, 2379 (1968); see also S. F. Mason and B. J. Norman, *Chem. Phys. Letters*, **2**, 22 (1968).
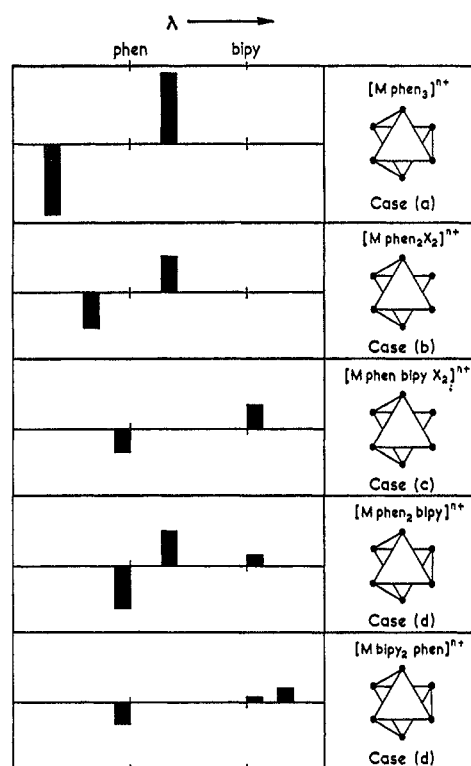

Figure 5. A diagrammatic representation of the predicted circular dichroism patterns for the various complexes shown in the absolute configurations which are all related to (−)-[Fe(phen)₃]²⁺. The lengths of the bars (which represent the values of the exciton rotational strengths) and their energy positions are quantitative and refer specifically to complexes containing various permutations of phen and bipy ligands. The same general pattern will hold for any permutation of other ligands provided the transition dipoles of these are directed along the octahedral edges. The calculated exciton rotational strength for a $[M(phen)_3]^{n+}$ complex is about ±12 × 10⁻³⁸ cgs and for a $[M(bipy)_3]^{n+}$ complex ±5 × 10⁻³⁸ cgs. The exciton interactions are: phen–phen = 950 cm⁻¹, bipy–bipy = 700 cm⁻¹, and phen–bipy = 850 cm⁻¹, and are calculated from the coulombic interactions between the transition monopoles of the ligands. These values are close to those found from experiment. The point-dipole–point-dipole interaction gives values which are 50% smaller, although the sense of the splitting is the same in both approximations.

In Figure 6 we show the absorption and circular dichroism spectra of the (+)-*cis*-[Ru(phen)₂(py)₂](ClO₄)₂ (py = pyridine) complex.[20] The two dominant circular dichroism bands in the 28,000-cm⁻¹ region conform with the expectations of the exciton theory (Table I, Figure 5) for the absolute configuration shown in the inset. The fact that the higher energy band is less intense than the lower energy exciton band is probably due to overlap with other transitions of the complex and to the possibility of mixing with other transitions of the system. Within the exciton formalism, mixing between nonidentical transitions is clearly brought out in the spectra of the (+)-[Ru(phen)₂bipy](ClO₄)₂ complex.[21] Figure 7 shows that, in the region of the long-axis-polarized transitions of phen and bipy, there are three strong circular dichroism bands, as is expected from exciton theory (Table I, Figure 5) for the absolute configuration shown in the inset. Although a similar pat-
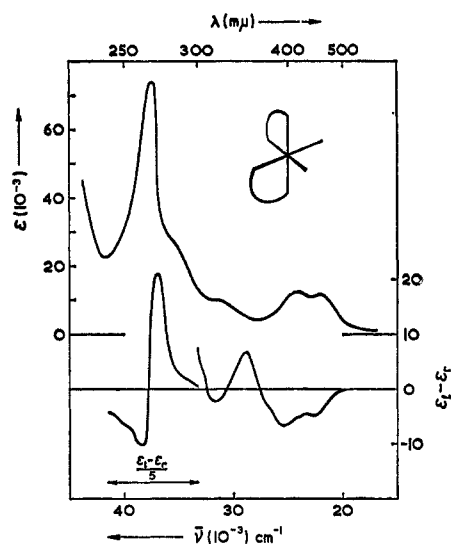
Figure 6. The absorption and circular dichroism spectra of (+)-cis-[Ru(phen)₂(py)₂](ClO₄)₂ in water solution and the predicted absolute configuration.
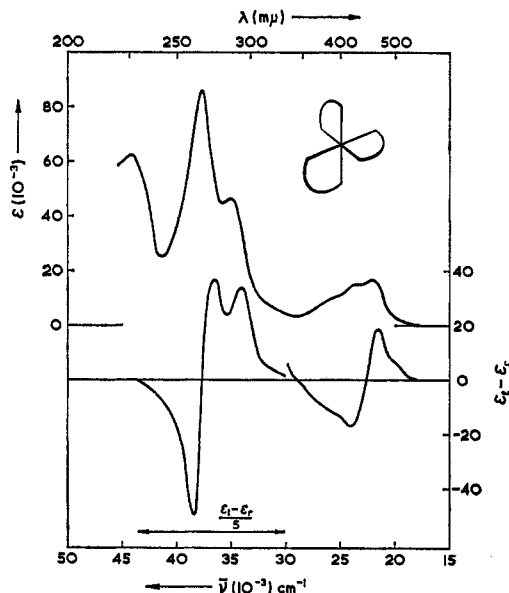

Figure 7. The absorption and circular dichroism spectra of (+)-[Ru(phen)₂bipy](ClO₄)₂ in water solution and the predicted absolute configuration.
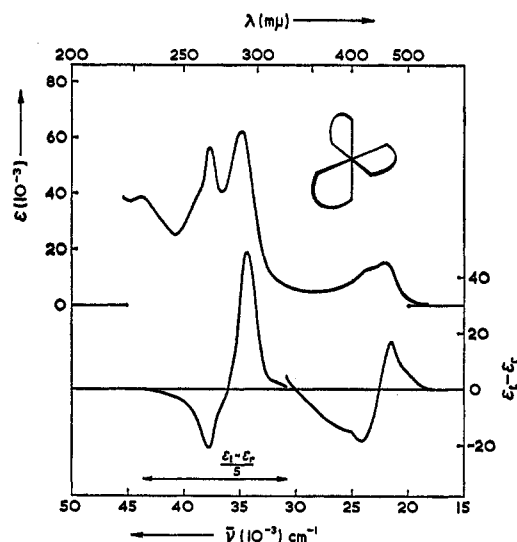

Figure 8. The absorption and circular dichroism spectra of (+)-[Ru(bipy)₂phen](ClO₄)₂ in water solution and the predicted absolute configuration.

the support provided by the absolute X-ray structure of the $(-)$-[Fe(phen)₃]²⁺ ion allow us to put forward a general rule for complexes of the type discussed here. *In the regions of the long-axis-polarized transitions of the ligands, the circular dichroism will appear strongly positive at lower energies and strongly negative at higher energies if the molecule has the absolute configuration related to* $(-)$-*[Fe(phen)₃]²⁺*. This rule is implicit in Table I and is illustrated in Figure 5.

The Formalism and Solutions

Suppose that the dissymmetric array has n residues (which may or may not be identical) with ground-state functions specified by χ_i. The total ground-state function for the assembly is given by

$$\Psi_0 = \chi_1\chi_2\chi_3\cdots\chi_i\cdots\chi_n$$

Assuming only single excitations, the local excited-state functions, Φ_i, are typified by

$$\Phi_i = \chi_1\chi_2\chi_3\cdots\chi_i'\cdots\chi_n$$

where the prime indicates an excited-state function of the ith residue. The total wave function, Ψ_j, corresponding to the jth excited state of the assembly, is expressed as a linear combination of the unperturbed singly excited-state functions, Φ_i, with the mixing coefficients, C_{ij}, associated with the ith function of the jth level

$$\Psi_j = C_{1j}\Phi_1 + C_{2j}\Phi_2 + \ldots + C_{ij}\Phi_i + \ldots + C_{nj}\Phi_j$$

where $j = 1, 2, 3, \ldots n$. The application of the variation theorem leads to the set of n simultaneous equations

$$\sum_{j=1}^{n}[H_{ij} - S_{ij}(H_{00} + E)]C_j = 0$$

$i = 1, 2, 3 \ldots n$, and $H_{ij} = \langle\Phi_i|H|\Phi_j\rangle$, $S_{ij} = \langle\Phi_i|\Phi_j\rangle$, H is the Hamiltonian of the system, and E is the appropriate energy. The term $H_{00} = \langle\Psi_0|H|\Psi_0\rangle$ refers to the

tern is expected for the (+)-[Ru(bipy)₂phen](ClO₄)₂ complex, experiment shows (Figure 8) only two clearly resolved circular dichroism bands in the regions of the long-axis-polarized transitions of the ligands. This arises from the fact that, as a numerical calculation will reveal, the two bands under the bipy absorption will be of the same sign and will be split by only about 1000 cm⁻¹. The important observation, however, is that the circular dichroism spectrum establishes that the phen and bipy transitions couple. In other words, the system belongs to case d and not to case b. So far no resolution of a complex belonging to case c has been reported.

Conclusion. A General Rule

The close semiquantitative agreement between theory and experiment—an agreement which is not greatly modified upon changing the metal atom—and

ground-state energy, including static multipole interactions. In order to obtain nontrivial solutions, the secular determinant is set to zero and the allowed energies found by solving for E

$$|H_{ij} - S_{ij}(H_{00} + E)| = 0$$

If normalized basis functions are used, $S_{ij} = 1$ when $i = j$ and, assuming zero overlap, $S_{ij} = 0$ when $i \neq j$. Provided it is assumed that the system is weakly coupled through electrostatic forces, the total Hamiltonian, H, of the system can be split up

$$H = \sum_{i=1}^{n} H_i + \sum_{i<j}^{n} \vartheta_{ij}$$

where H_i is the Hamiltonian of the ith residue and ϑ_{ij} is an electrostatic multipole interaction operator between the ith and jth residues. There are a number of ways by which this last term may be calculated, but it is usual to assume the point-dipole–point-dipole approximation which, although in many systems may give errors up to 50% in absolute magnitude, is generally reliable as far as the sense of the splitting is concerned. The point-dipole–point-dipole operator is

$$\vartheta_{ij} = \frac{1}{d_{ij}^3} \left\{ e\vec{R}_i \cdot e\vec{R}_j - \frac{3(e\vec{R}_i \cdot \vec{d}_{ij})(e\vec{R}_j \cdot \vec{d}_{ij})}{d_{ij}^2} \right\}$$

where $\vec{d}_{ij}$ is the vector distance between the transition point dipole moments of the ith and jth residues, e is the electronic charge, and $\vec{R}_i$ and $\vec{R}_j$ are the electronic position operators for the electrons involved in the transition of the ith and jth residues.

The rotational strength, $\Re$, of a transition between two stationary states φ_n and φ_m is defined as the pseudoscalar product

$$\Re = \mathrm{Im}\langle \varphi_n | \vec{M}_e | \varphi_m \rangle \cdot \langle \varphi_m | \vec{M}_\mu | \varphi_n \rangle$$

where $\vec{M}_e$ and $\vec{M}_\mu$ are the electric dipole and magnetic dipole operators, respectively, and Im means the imaginary part is taken. Thus the calculation of $\Re$ requires a knowledge of the electric transition dipole moment, $\vec{p} = \langle \varphi_n | \vec{M}_e | \varphi_m \rangle$, and the collinear magnetic transition dipole moment, $\vec{\mu} = \langle \varphi_m | \vec{M}_\mu | \varphi_n \rangle$. Within the exciton approximation these quantities can be calculated semiempirically.

The expression for the transition dipole moment, $\vec{p}_j$, for the excitation from the ground state, Ψ_0, to the jth-excited state, Ψ_j, of the assembly is given by

$$\vec{p}_j = \langle \chi_1\chi_2\chi_3\ldots\chi_i\ldots\chi_n | e\vec{R} | C_{1j}\Phi_1 + C_{2j}\Phi_2 + \ldots + C_{ij}\Phi_i + \ldots + C_{nj}\Phi_n \rangle$$

which, if orthonormal basis functions are used, reduces to

$$\vec{p}_j = \sum_{i=1}^{n} C_{ij} \langle \chi_i | e\vec{R}_i | \chi_i' \rangle = \sum_{i=1}^{n} C_{ij}\vec{p}_i$$

The corresponding dipole strength, D_j, is given by

$$D_j = \vec{p}_j \cdot \vec{p}_j = \sum_{i=1}^{n} \sum_{k=1}^{n} C_{ij}C_{kj}\vec{p}_i \cdot \vec{p}_k$$

The transition magnetic dipole moment can also be de-

rived on a similar semiempirical basis provided we assume that the transition dipole moment is produced by the displacement of a point charge. An electron of mass m and (negative) charge e with a linear momentum $\vec{p}$ rotating about a point at a distance $\vec{r}$ produces a magnetic moment $\vec{\mu}$ at right angles to the plane of rotation which is given by

$$\vec{\mu} = \frac{e}{2mc}(\vec{r} \times \vec{p})$$

where c is the velocity of light. The transition linear momentum and the transition dipole moment produced by the excitation of an electron between two stationary states φ_n and φ_m separated by a wave number frequency $\bar{\nu}$ are connected by the relationship

$$\vec{p} = \frac{i2\pi cm\bar{\nu}}{e} \langle \varphi_m | e\vec{R} | \varphi_n \rangle$$

whence the transition magnetic dipole moment is related to the electric transition dipole moment by

$$\vec{\mu} = i\pi\bar{\nu}(\vec{r} \times \langle \varphi_m | e\vec{R} | \varphi_n \rangle)$$

The expression for the magnetic moment, $\vec{\mu}_j$, produced by the transition between the ground state, Ψ_0, and the jth excited state, Ψ_j, of the assembly is therefore given by

$$\vec{\mu}_j = i\pi\sum_{i=1}^{n} C_{ij}\bar{\nu}_i(\vec{r}_i \times \langle \chi_i' | e\vec{R}_i | \chi_i \rangle)$$

$$\vec{\mu}_j = i\pi\sum_{i=1}^{n} C_{ij}\bar{\nu}_i(\vec{r}_i \times \vec{p}_i)$$

Hence, the rotational strength, $\Re_j$, for $\Psi_0 \rightarrow \Psi_j$ is given by

$$\Re_j = \mathrm{Im}\vec{p}_j \cdot \vec{\mu}_j = \pi\sum_{i=1}^{n} \sum_{k=1}^{n} C_{ij}C_{kj}\bar{\nu}_k\vec{p}_i \cdot (\vec{r}_k \times \vec{p}_k)$$

The details of these calculations for inorganic complexes may be found in ref 21. We should point out that for the nonidentical ligand cases there can be a problem of defining the origin for the magnetic moment, and hence the value of r in Table I is somewhat arbitrary. However, a dipole velocity calculation shows that the present definition of r gives the correct semiquantitative results for the present systems. The quantities in Table I which remain to be defined are the following. The terms V_{ij} are the interaction energies between the electric transition dipole moments and do not include the differences between the static multipole interactions. These have been set to zero. Using the point-dipole–point-dipole approximation the expressions for V_{12} (interaction between like molecules, e.g., phen–phen) and for V_{13} (interaction between unlike molecules, e.g., phen–bipy) are given by

$$V_{12} = \frac{\rho^2}{4d_{12}^3}$$

and

$$V_{13} = \frac{1}{d_{13}^3} \left\{ \frac{\rho_1\rho_3}{2} - \frac{3\rho_1\rho_3 r_1}{4(r_1 + r_3)^2} \right\}$$

where ρ is the transition dipole moment and d_{ij} is the effective distance between the electric point dipoles of adjacent ligand molecules in the complex. The mixing coefficients for case c are given by

$$C_A{}^- = C_B{}^+ = \frac{\Delta E_1 - \Delta E_2 - K}{2\left\{V_{12}{}^2 + \left(\dfrac{\Delta E_1 + \Delta E_2 - K}{2}\right)^2\right\}^{1/2}}$$

$$C_B{}^- = -C_A{}^+ = \frac{V_{12}}{\left\{V_{12}{}^2 + \left(\dfrac{\Delta E_1 + \Delta E_2 - K}{2}\right)^2\right\}^{1/2}}$$

where $K = \{(-\Delta E_1 - \Delta E_2)^2 + 4V_{12}{}^2 - 4\Delta E_1\Delta E_2\}^{1/2}$. Similarly the mixing coefficients for case d are

$$C_1{}^+ = -C_2{}^- = \frac{-\sqrt{2}V_{13}}{\left\{2V_{13}{}^2 + \left(\dfrac{\Delta E_1 + V_{12} - \Delta E_3 - L}{2}\right)^2\right\}^{1/2}}$$

$$C_2{}^+ = C_1{}^- = \frac{\Delta E_1 + V_{12} - \Delta E_3 - L}{2\left\{2V_{13}{}^2 + \left(\dfrac{\Delta E_1 + V_{12} - \Delta E_3 - L}{2}\right)^2\right\}^{1/2}}$$

where $L = \{(-\Delta E_1 - \Delta E_3 - V_{12})^2 - 4(\Delta E_1\Delta E_3 V_{12} - 2V_{13}{}^2)\}^{1/2}$. In these expressions ΔE_n refers to the transition energy of the nth ligand.

Reactions of Aromatic Compounds at High Temperatures

ELLIS K. FIELDS

Research and Development Department, Amoco Chemicals Corporation, Whiting, Indiana 46394

SEYMOUR MEYERSON

Research and Development Department, American Oil Company, Whiting, Indiana 46394

The behavior of aromatic compounds at high temperatures has intrigued chemists for many decades. In the early days of chemistry, as recorded in the first edition of Beilstein,[1] reagents were routinely passed through glowing porcelain or iron tubes and attempts were made to identify the products.

In 1929 Hurd[2] gathered in one volume the pyrolytic reactions of organic molecules. No researcher since has tried to write a comprehensive treatise similar to Hurd's; it would be a formidable task indeed. The reactions at high temperatures of a simple molecule such as toluene would appear predictable, involving scission of only C–H and C–C bonds. Yet in 1960 Badger and Spotswood[3] identified 23 products from toluene at 700°, and an additional 16 unidentified species were detected. Introduction of the heteroatoms O, S, and N vastly increases the complexity of thermal behavior.

A guide to introduce order and predictability into this complexity was obviously most desirable and necessary. A potential guide was found when we observed some striking parallels in the behavior of several compounds on pyrolysis and under electron impact in the mass spectrometer.[4-6] Such parallels had been re-ported earlier in a few scattered instances, for example, the similarity of the thermal retro-Diels–Alder reaction to that in the mass spectrometer.[7-11] However, the mechanistic implications and synthetic utility for organic chemists of relating thermal and mass spectral fragmentations were not widely realized until very recently.

Mass spectral fragmentation patterns have proven extremely useful to us, not only in explaining the course of some thermal reactions, but also in guiding our experimentation along new lines. Thus, for example, the partial mass spectrum of phthalic anhydride[14] and tentative structures of the ions in the main reaction sequence are as given in Table I. The large amount of $C_6H_4{}^+$ formed, most simply formulated as benzyne although the structure is not established, prompted us to try to duplicate this reaction thermally.

(7) S. Meyerson, J. D. McCollum, and P. N. Rylander, *J. Amer. Chem. Soc.*, **83**, 1401 (1961).

(8) K. Biemann, *Angew. Chem.*, **74**, 102 (1962); *Angew. Chem. Intern. Ed. Engl.*, **1**, 98 (1962).

(9) H. Audier, M. Fetizon, and W. Vetter, *Bull. Soc. Chim. France*, 1971 (1963).

(10) H. Budzikiewicz, J. I. Brauman, and C. Djerassi, *Tetrahedron*, **21**, 1855 (1965).

(11) R. C. Dougherty [*J. Amer. Chem. Soc.*, **90**, 5780 (1968)] has tried to define the relationships of mass spectral with pyrolytic and photolytic reactions by a perturbation molecular orbital interpretation.[12] Close parallels between mass spectral and pyrolytic decompositions have been rationalized by Brown, *et al.*, as reflecting parallelism of bond energies and vibrational modes in vibrationally excited neutral molecules and their ionized counterparts.[13]

(12) M. J. S. Dewar, *Tetrahedron Suppl.*, **8**, 75 (1966).

(13) R. F. C. Brown, G. E. Gream, D. E. Peters, and R. K. Solly, *Australian J. Chem.*, **21**, 2223 (1968).

(14) F. W. McLafferty and R. S. Gohlke, *Anal. Chem.*, **31**, 2076 (1959); S. Meyerson, *Record Chem. Progr.*, **26**, 257 (1965).

(1) "Beilstein's Handbuch der Organische Chemie," Vol. 5, Julius Springer, Berlin, 1922, *e.g.*, pp 185, 200, 284, 535.

(2) C. D. Hurd, "Pyrolysis of Carbon Compounds," Chemical Catalogue Co., New York, N. Y., 1929.

(3) G. M. Badger and T. M. Spotswood, *J. Chem. Soc.*, 4420 (1960).

(4) E. K. Fields and S. Meyerson, *Chem. Commun.*, 474 (1965).

(5) E. K. Fields and S. Meyerson, *J. Amer. Chem. Soc.*, **88**, 2836 (1966).

(6) S. Meyerson and E. K. Fields, *Chem. Commun.*, 275 (1966).